NUMERICAL MODELING OF LIQUID CO2 PHASE TRANSITION BLASTING BASED ON SPH ALGORITHM

by

Zhanbiao YANG [b,c], Yuejin ZHOU [a, *], Xiaoding XU [a, *], Wei YI [d], Mingpeng LI [a], and Xiaotong LI [a]

[a] State Key Laboratory for Geomechanics & Deep Underground Engineering, China University of Mining & Technology, Xuzhou, Jiangsu, China 221116;
[b] China Pingmei Shenma Group Institute of Energy and Chemical Industry, Pingdingshan, Henan, China 467000;
[c] State Key Laboratory of Coking Coal Exploitation and Comprehensive Utilization, Henan, China 467000;
[d] The Key Laboratory of Traffic and Transportation Security of Jiangsu Prainee, Huaiyin Institute of Technology, Huaian, Jiangsu 223003,China;

Abstract: Liquid CO_2 phase transition blasting is a physical blasting method to enhance permeability through liquid CO_2 phase transition expansion. To study the propagation criterion of fractures during blasting, the energy of phase transition blasting is evaluated through the thermodynamic equation by studying the action process of the liquid CO_2 blasting, thus obtaining the scope of the smash zone and crack zone as well as the propagation criterion of fractures under the effect of high-pressure gas. The gas blasting model for a coal body is established based on the SPH algorithm, thus obtaining the criteria for formation of the smash zone and for generation and propagation of the crack zone. Moreover, the radius of phase transition blasting is surveyed onsite by the peephole method. It is shown that the explosive energy of the MZL-51/2000 phase transition blasting equipment with a release pressure of 270 MPa is 1510 kJ. The coal body is crushed by the high-pressure CO_2 percussive drilling, forming the smash zone. Meanwhile, fractures are generated around the smash zone. With the expansion and migration of the gas, the fracture will further grow into a crack zone. The fracture inside the coal body goes through four states: rapid, slow, rapid, and then slow again. According to field surveys, the blasting radius of the MZL-51/2000 equipment with loaded liquid of 1.8 kg is approximately 3 m.

Key words: thermodynamics; phase transition blasting; gas blasting model; propagation of fracture

---

* Correspondence: Yuejin ZHOU: yuejinzh@163.com, Xiaoding XU: ding_xu@cumt.edu.cn

Introduction

Rock blasting is a destructive process that features large-scale deformation and high strain rate under the effects of a dynamic load. Considering the complicated action process, numerical modeling is adopted by numerous scholars in rock blasting studies across the world. The finite element software program LS-DYNA was adopted by Wang Zhiliang [1] to simulate the tensile damage of underground explosions for brittle rocks; the wave propagation of jointed rocks during explosion was simulated in [2]. A finite difference calculation program was developed in [3] and used for calculations of the development and surface peeling-off of the fractures generated in rock blasting; these calculation results were compared with those obtained via LS-DYNA for analysis. The degree of damage of the rock mass exploited through blasting was researched by Pan Pengfei, et al. [4] through the continuous–discontinuous element method. The influence of different explosive payloads on the underground blasting effect was simulated and analyzed by Wei, et al. [5] via the software program ANSYS-LSDYNA. Rock blasting was simulated by Ma, et al. [6] through the Johnson-Holmquist model, and some suggestions were proposed for the engineering application of rock blasting. The generation and propagation of fractures inside the rocks were simulated by Sivakumar [7] via the finite element method. Some achievements have been made in numerical modeling of rock blasting, but most are based on rock damage due to stress waves; the expansion and migration effect of high-pressure gas is barely considered, so it is difficult to obtain the propagation criterion and distribution pattern of fractures. The Smoothed Particle Hydrodynamics (SPH) algorithm, a mesh-free particle method, may overcome the deficiency of the finite element mesh method [8]. In this way, phenomena such as large-scale deformation, crushing and splashing of the materials during blasting and high-speed impact can be better simulated [9, 10]. In this paper, the blasting energy of phase transition blasting techniques is analyzed by means of the thermodynamic equation, and the propagation criterion of fractures during liquid CO_2 blasting is simulated and studied by using the SPH algorithm. Moreover, the radius of phase transition blasting is surveyed through onsite tests.

Technical Principle of Liquid CO2 Phase Transition Blasting

Liquid CO_2 Phase Transition Blasting Equipment

The liquid CO_2 phase transition blasting equipment mainly includes a blasting tube, activating device, constant-pressure shear sheet, release tube, etc, as shown in Figure 1.

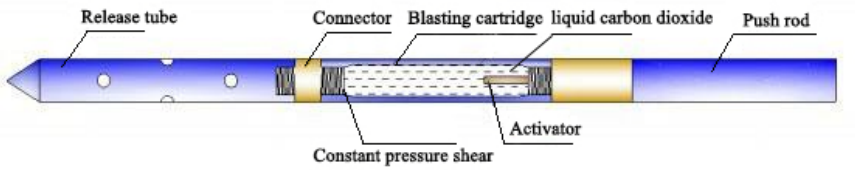

Figure 1. The main equipment of phase transition blasting

The liquid CO_2 is injected into the blasting tube through the filling system, and then the heating electrode is enabled by the initiation device. The chemicals inside the activating device are subject to rapid reaction after electrode heating, and then substantial heat

is released, leading to instantaneous gasification and expansion of the liquid CO_2. Once the pressure reaches the preset value, the constant-pressure shear sheet is fractured, and the gas erupts rapidly via the gas vent of the release tube to realize the objective of blasting by acting on the coal body.

Energy Analysis

Physical explosion is an extremely rapid energy release process, and the expansion of materials is converted into explosive energy by acting. The release form of energy includes the impact energy of high-pressure gas, energy of debris and residual deformation energy of vessels. Because the blasting tube is made of high-strength steel, the deformation is subtle, and most energy is released in the form of the impact of high-pressure gas.

In the case of phase transition blasting, the energy A of the entire system is evaluated by using the thermodynamic equation based on Helmholtz's free energy formula as follows [8]:

$$A = u - Ts \tag{1}$$

where T is temperature, s is energy, and u is internal energy.

The energy released from the explosion is expressed as

$$E = \int_1^2 pdV \cong -\Delta A \cong -\Delta u + T\Delta s \tag{2}$$

Entropy will not be changed during the expansion of high-pressure CO_2, so the energy released from the explosion is the decrement of internal energy. According to the gas state equation and law of thermodynamics, the internal energy u of unit mass of ideal gas is expressed as

$$u = \frac{1}{k-1}RT \tag{3}$$

where k is the heat ratio heat capacity, k=cp/cv; cp is the isobaric heat capacity; cv is the isochoric heat capacity; and cp-cv=R.

Consequently, the energy released from an explosion can be expressed as

$$E = \int_1^2 pdV \cong -\Delta u \cong \frac{1}{k-1}RT_1(1-\frac{T_2}{T_1}) \tag{4}$$

The change in entropy during gas expansion is expressed as

$$s_1 - s_2 = c_p \ln\frac{T_2}{T_1} - R\ln\frac{p_2}{p_1} \tag{5}$$

The change in isentropy is expressed as

$$\ln\frac{T_2}{T_1} = \frac{R}{c_p}\ln\frac{p_2}{p_1} \tag{6}$$

According to the definition of heat ratio heat capacity, $R/c_p=(k-1)/k$ can be obtained, and then

$$\frac{T_2}{T_1} = \left(\frac{p_2}{p_1}\right)^{\frac{k-1}{k}} \tag{7}$$

Therefore, the explosive energy equation is as follows:

$$E = \frac{1}{k-1} RT_1 (1 - \frac{T_2}{T_1}) = \frac{1}{k-1} p_1 V_1 \left[1 - \left(\frac{p_2}{p_1} \right)^{\frac{k-1}{k}} \right] \tag{8}$$

where E is the explosion energy of gas, kJ; p1 is the absolute pressure of gas inside the vessel, MPa; V1 is the volume of the vessel, L; k is the specific heat ratio of gas; p2 is the absolute pressure of the external environment, taking the standard barometric pressure; and R is the gas constant.

The MZL-51/2000 fracturing tube is 2 m long, with an outer diameter of 51 mm and a volume of 2 L. The loaded liquid is approximately 1.8 kg. According to Formula (8), where the release pressure calculated is 270 MPa, the blasting energy is 1510 kJ.

Analysis of Fracture Propagation Mechanism

Analysis on Fracture Propagation under the Effect of a Stress Wave

During propagation of the stress wave, the peak value of the wave is under constant attenuation, the rules of which can be expressed as

$$\sigma_{rd} = P \left(\frac{r_0}{r} \right)^{\alpha} \tag{9}$$

where P is the initial incident pressure of the wave; r is the distance from some point of the rock to the center of boreholes; r_0 is the radius of the borehole; σrd is the radial stress in some point of the rock; and α is the attenuation coefficient of the stress wave, $\alpha = 2\text{-}\mu / (1-\mu)$.

At the boundary of the smash zone, the speed of the shock wave is attenuated into that of the stress wave, and the particle velocity ur is expressed as

$$u_r = \frac{c_p}{1+k} \tag{10}$$

where k is the isentropic coefficient.

According to the law of the conservation of momentum, the peak pressure Prmax calculated at the boundary of the smash zone is expressed as

$$P_{r\max} = \rho c_p u_r \tag{11}$$

The calculated radius R0 of the smash zone of the coal body is expressed as

$$R_0 = r_0 \sqrt[\alpha]{\frac{P(1+k)}{\rho c_p^{\,2}}} \tag{12}$$

Under the effect of the shock wave, the coal body will be subject to damage to different extents. The attenuation coefficient αD of the stress wave considering the damage can be expressed as

$$\alpha_D = \frac{\alpha}{1-D} \tag{13}$$

where D is the damage factor, and α is the attenuation coefficient of the stress wave in the undamaged coal body.

The relationship between the dynamic radial stress σrd and the dynamic circumferential stress σθd is expressed as

$$\sigma_{\theta d}=\frac{\mu}{1\text{-}\mu}\sigma_{rd} \tag{14}$$

Considering the influence of damage on the strength of the coal body, the dynamic tensile strength of rocks can be expressed as σtd(1-D), so

$$\sigma_{td}\left(1-D\right)=P\left(1-2b^2\right)\left(\frac{r_0}{r}\right)^{\alpha_D} \tag{15}$$

The calculated radius R1 of the crack zone is expressed as

$$R_1=r_0\sqrt[\alpha_D]{\frac{P\left(1-2b^2\right)}{\sigma_{td}\left(1-D\right)}} \tag{16}$$

Analysis of the Fracture Propagation under the Effect of High-Pressure Gas

The acting duration of high-pressure gas on the coal body due to expansion inside the borehole is at least orders of magnitude over that of the stress wave. Because the pressure of HP gas is relatively stable, the action process can be deemed as a quasi-static process [11]. The stress intensity factor KI of the macro fractures under the effect of HP gas is expressed as

$$K_I=2\sqrt{\frac{a+r_0}{\pi}}\int_0^{a+r_0}\frac{P_g\left(x,t\right)}{\sqrt{\left(a+r_0\right)^2-x^2}}dx \tag{17}$$

where $P_g(x,t)$ is the pressure distribution of high-pressure gas on the surface of macro fractures at time t, and a is the length of macro fractures under the effect of ground stress, as shown in Figure 2.

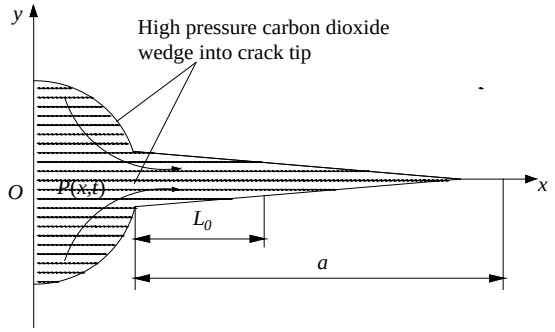

Figure 2. The model of fracture propagation driven by HP gas

The relationship between the pressure distribution of high-pressure gas on the surface of macro fractures and the time variation is simplified as

$$P_g\left(x,t\right)=P\left(t\right)e^{-\alpha x} \tag{18}$$

where P(t) is the pressure of HP gas inside the borehole, MPa, and α is the attenuation coefficient of stress.

During liquid CO_2 phase transition blasting, the length of fractures is far greater than the radius of the borehole, so the stress intensity factor K_I of the macro fractures under the effect of high-pressure gas can be simplified as follows if r_0=0:

$$K_I=2\sqrt{\frac{a_0}{\pi}}\int_0^{a_0}\frac{P_g\left(x,t\right)}{\sqrt{a^2-x^2}}dx=\pi P\left(t\right)e^{-ab}\sqrt{\frac{a}{\pi}} \tag{19}$$

The development of the fracture tip is the consequence of constant accumulation of damage, so the effective stress intensity factor is defined to reflect the dynamic propagation process of fractures.

The effective stress intensity factor considering damage is expressed as

$$K_I^* = \frac{\pi P(t) e^{-ab} \sqrt{\frac{a}{\pi}}}{1\text{-}D} \sqrt{\quad} \tag{20}$$

Assuming that the dynamic fracture toughness of the coal body is KDIC, the stable propagation conditions of fractures can be expressed as

$$K_I^* \geq K_{DIC} \tag{21}$$

The SPH Algorithm Theory

The SPH algorithm—i.e., the smoothed particle hydrodynamics algorithm—is a Lagrange mesh-free algorithm proposed in the international community in recent years[12].

The equation of the SPH algorithm is generally carried out in two steps. The first step is the kernel approximation of the field function—namely, approximating the field function via an integral representation.

$$f(x) \approx \int_\Omega f(x') W(x - x', h) d\ ' \tag{22}$$

where h is the smoothing length, determining the influence scope of $W(x - x', h)$.

The second step is to separate the system into limited particles with independent mass and space, so the continuous integral representation of the SPH kernel approximation can be converted into a dispersed mode solving the sum of all particles in the domain.

$$f(x) = \int_\Omega f(x') W(x - x', h) d\ ' \approx \sum_{j=1}^{N} f(x_j) W(x - x_j, h) \frac{m_j}{\rho_j} \tag{23}$$

where N is the total number of particles in the area requiring solution; ρj is the density of particle j; and mj is the mass of particle j.

Constitutive Selection

HJC Constitutive Model

The HJC model is composed of an equivalent strength model, state equation, and damage model [13]. The HJC equivalent strength model described by dimensionless equivalent stress can be expressed as follows:

$$\sigma^* = \left[A(1 - D) + BP^{*N} \right] \left(1 + C \ln \dot{\varepsilon}^* \right) \tag{24}$$

where σ^* is the dimensionless equivalent stress, P^* is the dimensionless pressure, P is the hydrostatic pressure, $\dot{\varepsilon}^*$ is the dimensionless strain rate, D is the damage factor, and A, B, C, and N are material constants.

The state equation is expressed in piecewise terms, indicating the changes in hydrostatic pressure with volumetric strain. The compression process is divided into three states: the elastic stress state, plastic state, and permanent densification state, as shown in Figure 3. P is hydrostatic pressure, μ is the volumetric strain of the rock, Ke is the bulk modulus of elasticity, μcrush is the elastic limit volumetric strain, Pcrush is the hydrostatic pressure when the rock reaches its elastic limit, $K_{crush} = (P_{lock} - P_{crush}) / (\mu_{lock} - \mu_{crush})$, $\overline{\mu}$ is the corrected volumetric strain, μlock is the corresponding volumetric strain of the permanent densification limit, and K_1, K_2, and K_3 are pressure constants.

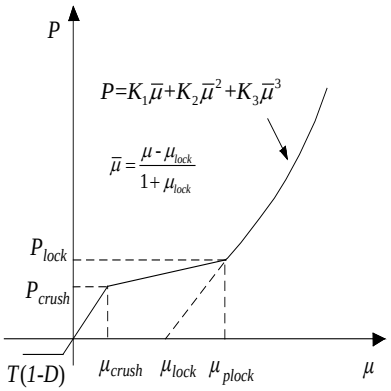

Figure 3. Changes in Hydrostatic Pressure with Volumetric Strain

Damage variable D is obtained through the accumulation of equivalent plastic strain and plastic volumetric strain, whose damage evolution equation is as follows:

$$D=\sum \frac{\Delta \varepsilon_p + \Delta \mu_p}{\varepsilon_p^f + \mu_p^f} \tag{25}$$

By leveraging the tests of uniaxial compression, tensile splitting strength, and other tests for coal, the physical and mechanical parameters of coal are obtained as follows: elastic modulus E is 2.47 GPa, Poisson's ratio μ is 0.3, compressive strength fc is 16.32 MPa, tensile strength T is 1.34 MPa, and density ρ0 is 1400 kg/m3. In addition, shear modulus G and bulk modulus Ke of coal can be obtained as

$$G = \frac{E}{2(1+\mu)} = 0.95\text{GPa} \quad \text{and} \quad K_e = \frac{E}{3(1\text{-}2\mu)} = 2.06\text{GPa}$$

The corresponding volumetric strain and hydrostatic pressure when the material reaches its elastic limit can be obtained according to the following equations:

$P_{\text{crush}} = f_c/3 = 3.44\text{MPa}$; $\mu_{\text{crush}} = P_{\text{crush}}/K_e = 0.0017$.

At dimensionless tension $T^* = T/f_c = 0.11$, damage factor $D_1 = 0.01/(1/6+T^*) = 0.036$. Damage factor D2 has little influence on the model results [14]. Therefore, D2 = 1 according to the literature [14].

Xie [15] indicated that the densification density of the coal rock test $\rho_{\text{grain}} = 1631\text{kg/m}^3$, and the volumetric strain of the densification limit $\mu_{\text{lock}} = \rho_{\text{grain}}/\rho_0 - 1 = 0.14$. K1, K2, and K3 can be determined according to the Hugoniot shock test or taken from the literature [16] in the absence of test data: K1 = 85 GPa, K2 = −171 GPa, and K3 = 208 GPa. According to Xie Beijing [15], take Plock = 1 GPa, $A=0.4$, $B=0.7$, $C=0.005$, and $N=0.5$.

State Equation of High-Pressure Gas

The JWL state equation may describe an explosion without chemical reaction and accurately reflect the expansive driving process of blasting products [17]. Therefore, the following JWL state equation can be used as the CO_2 state equation. The JWL state equation is

$$P = A\left(1-\frac{\omega}{R_1 V}\right)e^{-R_1 V} + B\left(1-\frac{\omega}{R_2 V}\right)e^{-R_2 V} + \frac{\omega E}{V} \tag{26}$$

where P is the pressure of blasting products, V is the relative specific volume, E is the internal energy of blasting products per unit volume, and A, B, R_1, R_2, and ω are parameters to be determined.

When the release pressure of the constant-pressure shear sheet is 270 MPa, the energy released from the explosion of liquid CO_2 fracturing equipment is approximately 1510 kJ. With reference to the state equation of blasting products generated by TNT, taking A = 3.73×1011, B = 3.75×109, R1 = 4.15, R2 = 0.9, ω = 0.35 and E = 6109, the high -pressure radius gas is 6 mm.

Numerical Modeling of Phase Transition Blasting

Liquid CO_2 blasting of a coal body is a highly nonlinear dynamic process at a high strain rate. It is easy to generate mesh distortion and terminate the calculation using a conventional Lagrange algorithm. Meanwhile, considering the expansion and migration of high-pressure gas, the SPH algorithm is adopted to model the liquid CO_2 blasting process of a coal body.

In the numerical modeling, the geometric size of the coal body is 10 m × 10 m, and there is a round borehole with a diameter of 75 mm in the center, as shown in Figure 4. The constitutive model is the HJC model and is added to the maximal tension stress failure criterion. Both the coal body and high-pressure gas are modeled using the SPH algorithm, and their numbers of particles are 110,764 and 592, respectively. The monitoring points are set at 0.3 m, 0.5 m, 1 m, 1.5 m, 2 m, and 2.5 m from the borehole on the right.

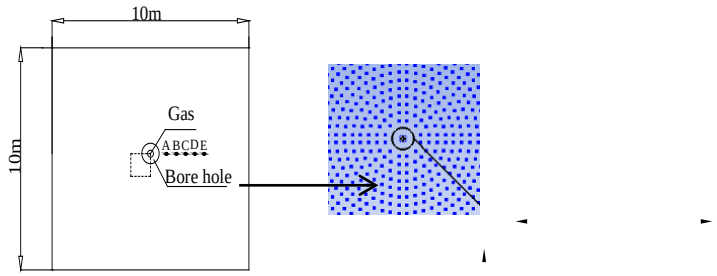

Figure 4. Numerical Model of Liquid Carbon Dioxide Blasting

The modeling results of fracture distribution of the coal body after liquid carbon dioxide blasting are shown in Figure 5.

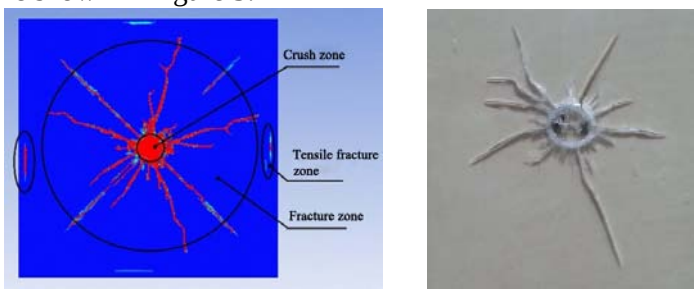

(*a*) Numerical Modeling of Fracture Distribution (*b*) Test of Fracture Distribution

Figure 5. Final Distribution Pattern of Blasting Fractures

The complete fracture evolution process in the phase transition blasting process is shown in Figure 6.

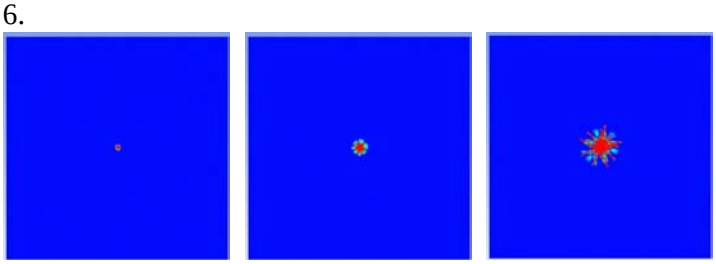

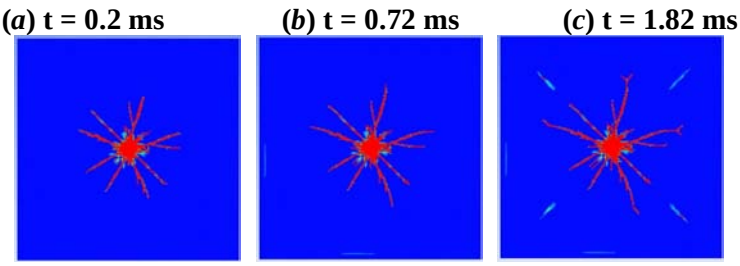

Figure 6. Complete Evolution Process of Blasting Fractures

The reflected stress wave generates a tension effect on the fractures, and the fracture propagation speed changes dramatically, as shown in Figure 7.

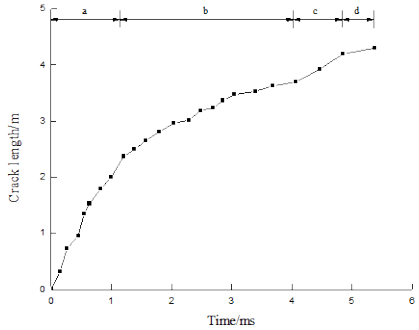

Figure 7. Relationship between Fracture Length and Time

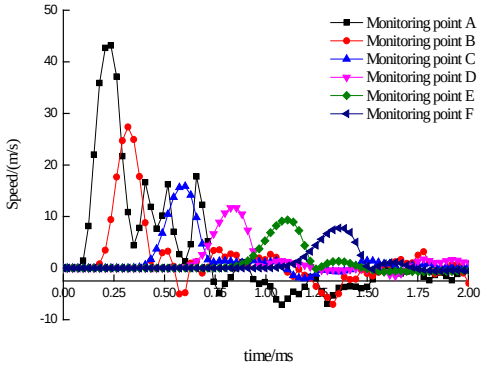

Figure 8. Relationship between Speed at Monitoring Point and Time

Figure 8 shows that the speed of the particles near the borehole increases rapidly at the early stage of blasting. Figure 9 indicates the relationship between the monitoring point position and the peak speeds at monitoring points and their corresponding time points.

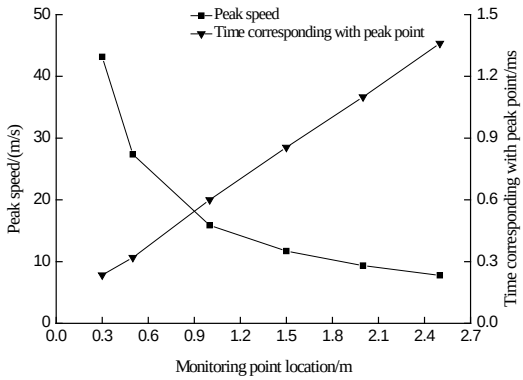

Figure 9. Relationship between the Monitoring Point Position and the Peak Speeds at Monitoring Points and Their Corresponding Time Points

Survey and Test of Blasting Radius

A radius survey and test were carried out in the air return channel of the working surface. Boreholes with a diameter of 75 mm and depth of 60 m were arranged at either side of the undrained mining area. Moreover, three holes were drilled at the left and right sides of the blasting hole as peepholes. The distances from the peepholes to the blasting hole were set to 1.5 m, 2 m, 3 m, 3.5 m, 4 m, and 5 m in sequence. The layout of boreholes is shown in Figure 10.

The loaded liquid of the MZL-51/2000 fracturing equipment was 1.8 kg, and the release pressure of the constant-pressure shear sheet was 270 MPa. Linkages within the blasting hole and the blasting equipment were uniformly arranged at a ratio of 1:1, with a hole sealing length of 15 m.

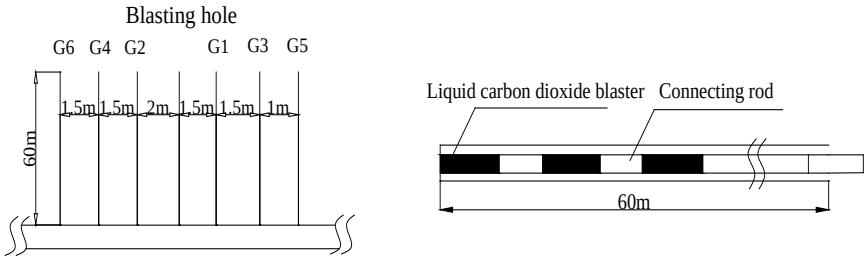

Figure 10. Schematic Diagram for Layout of Boreholes

The peeping instrument was used to observe the crushing of the coal bed inside the boreholes. The observation results of boreholes G3 and G4 are shown in Figure 11.

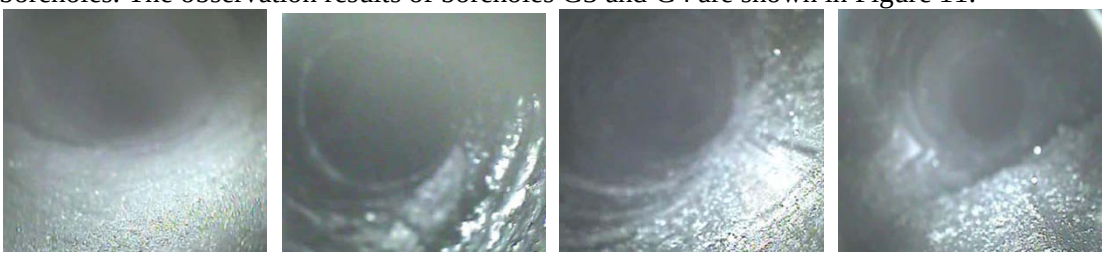

(*a*) Before blasting of G3 (*b*) After blasting of G3(*c*) Before blasting of G4 (*d*) After blasting of G4

Figure 11. Borehole View

It can be seen in Figure 11 that borehole G3 has a smooth wall before phase transition blasting, and there are only a few small cracks in the coal body.

Conclusions

Through studying the action process of liquid CO_2 blasting, the energy of phase transition blasting is evaluated using a thermodynamic equation, and an explosion energy equation is established. The explosion energy of MZL-51/2000 liquid CO_2 phase transition blasting equipment at 270 MPa is calculated to be 1510 kJ.

According to the form of the damage, the smash zone, crack zone, and tension crack zone are roughly formed after coal body blasting. Liquid CO_2 leads to the formation of a limited smash zone on the inner wall of the borehole under the action of instant thermal expansion. Subsequently, under the joint action of the stress wave and high-pressure gas, the crack zone connected with the smash zone is formed. The stress wave reflected from the boundary is converted into a tensile wave, which continues to generate tension cracks at the boundary of the coal body.

The phase transition blasting of the coal body is modeled based on the SPH algorithm to simulate the liquid carbon dioxide phase transition blasting, analyze the formation mechanism of cracks in the blasting process, and obtain the laws for formation of the smash zone around the borehole as well as generation and expansion of the crack zone.

The radius of phase transition blasting is surveyed by using the peephole method. The blasting radius of the MZL-51/2000 phase transition blasting equipment with 1.8 kg of

loaded liquid is approximately 3 m.

Acknowledgement

This research is supported by the National Key Research and Development Program of China (2018YFC0604705) and the National Natural Science Foundation of China (51874289) and the Fundamental Research Funds for the Central Universities (2018ZDPY05).

Reference

[1] Wang, Z., Numerical analysis of blast-induced wave propagation and spalling damage in a rock plate, *International Journal of Rock Mechanics & Mining Sciences*, 45 (2008), 4, pp. 600-608

[2] Gasmi, H., Numerical Homogenization of Jointed Rock Masses Using Wave Propagation Simulation, *Rock Mechanics & Rock Engineering*, 47 (2014), 4, pp. 1393-1409

[3] Wang, Z., *et al.*, Numerical analysis of blast-induced wave propagation and spalling damage in a rock plate, *International Journal of Rock Mechanics and Mining Sciences*, 45 (2008), 1, pp. 600-608

[4] Pan, P., *et al.*, Numerical Study on Damage and Fracture Degree of Rock Mass Induced by Blasting Mining, *Metal Mine*, 6 (2016), 1, pp. 1-7

[5] Wei, X., *et al.*, Numerical simulations of rock mass damage induced by underground explosion, *International Journal of Rock Mechanics and Mining Sciences*, 46 (2009), 1, pp. 1206-1213

[6] Ma, G., *et al.*, Numerical simulation of blasting-induced rock fractures, *Int J Rock Mech Mining Sci*, 45 (2008), 3, pp. 966-975

[7] Sivakumar, G., *et al.*, Finite element simulation of crack initiation and propagation in rocks, *Rock Engineering and Rock Mechanics*, 41(2014), 8, pp. 829-834

[8] Devuyst, T., *et al.*, Coupling between meshless and finite element methods, *International Journal of Impact Engineering*, 31*(2005)*, 8, pp. 1054-1064

[9] Campbell, J., *et al.*, A contact algorithm for smoothed particle hydrodynamics, *Computer Methods in Applied Mechanics and Engineering*, 184(2000), 1, pp. 49-65

[10] Xue, Y., *et al.*, An elastoplastic model for gas flow characteristics around drainage borehole considering post-peak failure and elastic compaction, *Environmental Earth Sciences*, 77 (2018), 19, pp. 669

[11] Li, C., *et al.*, Experiment of dynamic property and transient magnetic effects of coal during deformation and fracture, *Journal of Coal Science and Engineering (China)*, 6 (2012), 3, pp. 258-261

[12] Chu, H., *Theoretical and experimental studies on coal blasting action mechanism*, Henan Polytechnic University, 2011.

[13] Xue, Y., *et al.*, Evaluation of the Non-Darcy Effect of Water Inrush from Karst Collapse Columns by Means of a Nonlinear Flow Model, *Water*, 10 (2018), 9, pp. 1234

[14] Paine, A., Please, C., An Improved Model of Fracture Propagation by Gas during Rock Blasting-Some Analytical Results, *International Journal of Rock Mechanics and Mining Sciences,* 31 (1994), 6, pp. 699-706

[15] Xie, B., *Experimental research on characteristics of coal impact damage dynamics and magnetic field*, China University of Mining and Technology (Bejing), 2013
[16] Pei, X., *Numerical Simulation for Compressive Residual Stress and Surface Morphology of Shot-peening Based on SPH Method*, Shandong University, 2013
[17] Li, Y., *The Numerical Simulation Researches on the Law of Improving the Permeability of Low Permeability Coal Seam by Air Blasting*, Liaoning Technical University, 2015

Paper submitted: May 1, 2018
Paper revised: September 20, 2018
Paper accepted: December 15, 2018